MOLECULAR AND CELLULAR BIOLOGY, Feb. 2010, p. 1077–1087 Vol. 30, No. 4
0270-7306/10/$12.00 doi:10.1128/MCB.01067-09

Rab13 Regulates Neurite Outgrowth in PC12 Cells through Its Effector Protein, JRAB/MICAL-L2[▽]

Ayuko Sakane,[1] Kazufumi Honda,[2] and Takuya Sasaki[1]*

Department of Biochemistry, Institute of Health Biosciences, University of Tokushima Graduate School, Tokushima 770-8503, Japan,[1] and Chemotherapy Division and Cancer Proteomics Project, National Cancer Center Research Institute, Tokyo 104-0045, Japan[2]

Received 11 August 2009/Returned for modification 14 September 2009/Accepted 2 December 2009

Neurite outgrowth is the first step in the processes of neuronal differentiation and regeneration and leads to synaptic polarization and plasticity. Rab13 small G protein shows an increased mRNA expression level during neuronal regeneration; it is therefore thought to be involved in this process. We previously identified JRAB (junctional Rab13-binding protein)/MICAL-L2 (molecules interacting with CasL-like 2) as a novel Rab13 effector protein. Here, we show that Rab13 regulates neurite outgrowth in the rat pheochromocytoma cell line PC12 through an interaction with JRAB/MICAL-L2. The expression of JRAB/MICAL-L2 alone inhibits neurite outgrowth, whereas coexpression of the dominant active form of Rab13 rescues this effect. We also demonstrate an intramolecular interaction between the N-terminal calponin-homology (CH) and LIM domains of JRAB/MICAL-L2 and the C-terminal coiled-coil domain. Finally, we show that the binding of Rab13 to JRAB/MICAL-L2 stimulates the interaction of JRAB/MICAL-L2 with actinin-4, an actin-binding protein, which localizes to the cell body and the tips of the neurites in PC12 cells. These results suggest that Rab13 and JRAB/MICAL-L2 may act to transfer actinin-4 from the cell body to the tips of neurites, where actinin-4 is involved in the reorganization of the actin cytoskeleton which results in neurite outgrowth.

Neuronal cells are symmetrically shaped in the very early stages of development. When fully developed, they are asymmetrical, with one long thin axon. The polarization of cell morphology and the creation of synaptic contacts via elongation of the axon and dendrites during development is a crucial event in the process of neuronal differentiation and regeneration and is called neurite outgrowth (18, 23). During neurite outgrowth, neuronal cells are stimulated to extend processes by a multitude of extracellular signals and eventually establish synaptic contacts by which they are able to communicate with one another. It is clear that the process of neurite outgrowth requires massive transport of proteins such as receptors for extracellular signaling molecules or neuronal cell adhesion molecules to extensions of the plasma membrane, as well as replenishment of plasma membrane lipids. However, little is known of the details of the membrane traffic machinery involved in these processes.

In contrast, the role of cytoskeletal dynamics in neurite outgrowth is well established. Overwhelming evidence accumulated in recent years indicates that the Rho family of small G proteins play a critical role in the regulation of the actin cytoskeleton (5, 6, 8, 20). The Rho family members RhoA, Rac1, and Cdc42 have been investigated most extensively. They participate in the reorganization of the actin cytoskeleton into distinct structures including lamellipodia, filopodia, and stress fibers (6). Reorganization of the actin cytoskeleton at the tips of the developing neurites pushes the leading cell edge forward, indicating that actin cytoskeletal dynamics are necessary for neurite outgrowth (3, 13).

The Rab family of small G proteins play important roles in mediating vesicular membrane traffic in eukaryotic cells (20, 25). More than 60 mammalian Rab proteins have been identified and characterized. They are localized to different cellular compartments and control distinct transport systems. We have previously shown that Rab13, a member of the Rab family, and its effector protein, JRAB (junctional Rab13-binding protein)/MICAL-L2 (molecules interacting with CasL-like 2), are involved in the transport of the cell adhesion molecules occludin and claudins to the tight junctional area in epithelial cells (14, 16, 21, 24). Moreover, we identified actinin-4 as a JRAB/MICAL-L2-binding protein and found that actinin-4 links JRAB/MICAL-L2 to filamentous actin (F-actin) (15). These data allowed us to speculate that Rab13 might be responsible for the delivery of cell adhesion molecules or receptors for extracellular signals to the tips of the neurites, and that cross talk between Rab13-JRAB/MICAL-L2-mediated membrane traffic and actin dynamics is tightly coupled to the formation of neurites.

In the present study, we have analyzed the role of Rab13-JRAB/MICAL-L2 in neurite outgrowth using the rat pheochromocytoma cell line PC12, which differentiates into neuronal cells and extends neurites after addition of nerve growth factor (NGF). Our data demonstrate the coordination of Rab13-JRAB/MICAL-L2-mediated membrane traffic with actin cytoskeletal rearrangement and suggest that this interaction might integrate membrane traffic and cytoskeletal dynamics during the process of neurite outgrowth.

MATERIALS AND METHODS

Plasmid construction. The cDNAs encoding wild-type Rab13 (Rab13WT), and the dominant active and dominant-negative Rab13 mutant proteins (Rab13DA and Rab13DN) were subcloned into pEGFP-C1 or pDsRed-C vec-

* Corresponding author. Mailing address: Department of Biochemistry, Institute of Health Biosciences, University of Tokushima Graduate School, 3-18-15 Kuramato-cho, Tokushima 770-8503, Japan. Phone: 81-88-633-9223. Fax: 81-88-633-9227. E-mail: sasaki@basic.med.tokushima-u.ac.jp.

▽ Published ahead of print on 14 December 2009.

tor, using the BamHI restriction sites. Construction of pCIneo-Myc-JRAB-F (full length of mouse JRAB) and -JRAB mutants was performed as reported previously (21) except for pCIneo-Myc-JRABΔCT and -JRABΔCC. JRABΔCT (amino acids 1 to 912) cDNA was generated by PCR using pCIneo-Myc-JRAB-F as a template and subcloned into the pCIneo-Myc vector. To obtain JRABΔCC cDNA, the coding regions for amino acids 1 to 805 and 913 to 1009 were amplifying by PCR using pCIneo-Myc-JRAB-F as a template. The products were ligated and subcloned into the pCIneo-Myc vector. For the production of green fluorescent protein (GFP)- or DsRed-fusion constructs, the cDNAs of JRAB-F and JRAB mutants were subcloned into pEGFP-C1 or pDsRed-C using the same restriction sites. Construction of pCIneo-Myc-actinin-4 was done as described previously (15). All plasmids constructed in the present study were sequenced by using an ABI Prism 3100 genetic analyzer (Applied Biosciences, Foster City, CA).

Antibodies. The rabbit polyclonal anti-JRAB/MICAL-L2 antibody was raised against GST-JRAB-C and purified as described previously (21). Mouse anti-Myc antibody (9E10) was produced from hybridoma, which was obtained from the American Type Culture Collection (Manassas, VA), and mouse anti-β-tubulin antibody from Sigma-Aldrich (St. Louis, MO). Rabbit anti-green fluorescent protein (anti-GFP) and mouse anti-GFP antibodies and rhodamine phalloidin were purchased from Invitrogen (Carlsbad, CA). Production of the rabbit polyclonal antibody against actinin-4 was described previously (7).

Cell culture and transfection. PC12 cells were cultured in Dulbecco's modified Eagle's medium (DMEM) with 10% fetal bovine serum (FBS), 5% horse serum, 100 U of penicillin/ml, and 100 mg of streptomycin/ml and were maintained at 37°C in a water-saturated atmosphere of 90% air and 10% CO_2. COS7 cells were cultured in DMEM with 10% FBS, 100 U of penicillin/ml, and 100 mg of streptomycin/ml and were maintained at 37°C in a water-saturated atmosphere of 90% air and 10% CO_2. PC12 and COS7 cells were transfected by using the Lipofectamine 2000 transfection reagent (Invitrogen) according to the manufacturer's instructions.

Pulldown assays. COS7 cells were seeded at a density of 5×10^5 cells on 60-mm dishes and transfected the following day with 4 μg of each plasmid using the Lipofectamine 2000. After a 48-h incubation at 37°C, the cells were washed once and scraped from the dishes in phosphate-buffered saline (PBS). The cells were lysed in 300 μl of buffer A [10 mM Tris-HCl (pH 8), 1 mM EDTA, 1% (wt/vol) Nonidet P-40, 150 mM NaCl, 10 μM (4-amidinophenyl)-methanesulfonyl fluoride]. The cell lysates were centrifuged at 4°C for 7 min at 16,100 × *g*, and each supernatant was incubated for 90 min at 4°C with 2 μg of purified GST-JRAB-C attached to glutathione-Sepharose beads. The beads were then washed with buffer A three times and resuspended in sodium dodecyl sulfate (SDS) sample buffer. Comparable amounts of the proteins that remained associated with the beads were separated by SDS-PAGE. The fraction of Myc-JRAB-F or -JRAB mutants bound to the affinity column was determined by immunoblotting with an anti-Myc antibody.

Immunocytochemistry. PC12 cells were seeded at a density of 4×10^5 cells on a poly-L-lysine-coated 35-mm dish (Corning, Corning, NY) and transfected the following day with various DNA plasmids. After 48 h of incubation, the cells were fixed with 4% formaldehyde in PBS at room temperature for 20 min. The cells were then incubated in 5% goat serum and 0.1% Triton X-100 in PBS for 30 min. Next, they were incubated with primary antibodies for 1 h, followed by incubation with Alexa 488-, Alexa 546-, or Pacific Blue-conjugated secondary antibodies (Invitrogen) for 1 h. F-actin was labeled with rhodamine phalloidin (Invitrogen). The stained cells were observed under an Axiovert 200M imaging microscope (Carl Zeiss, Jena, Germany), LMS Pascal confocal-scanning microscope (Carl Zeiss) or an A1 confocal laser-scanning microscope (Nikon, Tokyo, Japan).

RNA interference (RNAi). The 25-mer small interfering RNA (siRNA) duplex targeting rat JRAB/MICAL-L2 (GenBank/EMBL/DDBJ accession no. XM_221956), as well as the control nonsilencing siRNA duplex, was obtained from Invitrogen and transfected by using Lipofectamine 2000 reagents (Invitrogen) according to the manufacturer's instructions. The target sequences were as follows for rat JRAB/MICAL-L2: #1, 5′-GATCAGACCAGGAGCTGTAAGGAGA-3′; #2, 5′-TCATGGTGGACTGGTTCCGGCTTAT-3′; and #3, 5′-GGCGTGAATCGGAACTCATGTACAA-3′. To prepare miRNA against JRAB/MICAL-L2, the miRNA sequence of JRAB/MICAL-L2 was designed based on the target sequence of #3 siRNA and inserted into pcDNA6.2-GW/EmGFP-miR vector (Invitrogen). This plasmid as well as the control plasmid, pcDNA6.2-GW/EmGFP-miR-neg control plasmid (Invitrogen) was also transfected by using Lipofectamine 2000 reagents.

Quantitative real-time reverse transcription-PCR (RT-PCR). Total RNA was extracted from freshly prepared PC12 cells by using BioRobot EZ1 with a Universal Tissue kit (Qiagen, Valencia, CA) and reverse transcribed by using a QuantiTect reverse transcription kit (Qiagen) according to the manufacturer's specifications. Real-time PCR analysis was performed with an ABI 7500 real-time PCR system (Applied Biosystems) using TaqMan gene expression assays according to the manufacturer's instructions. To measure siRNA-induced knockdown of JRAB/MICAL-L2, the comparative C_T method ($\Delta\Delta C_T$) for relative quantification was used.

Immunoprecipitation. PC12 cells or transfected COS7 cells were washed twice with PBS and lysed in buffer A. After removal of the cell debris, the lysates were incubated with an anti-JRAB/MICAL-L2 antibody bound to protein A-Sepharose FF (GE Healthcare Biosciences, Piscataway, NJ). The beads were washed three times with the lysis buffer and boiled in SDS sample buffer. These samples were used for the immunoblotting.

Immunoblotting. The cell lysates or the immunoprecipitates were subjected to SDS-PAGE. The separated proteins were transferred to the membrane by using the iBlot gel transfer system (Invitrogen). The membranes were probed with specific primary antibodies and then with horseradish peroxidase-coupled secondary antibodies (Jackson Immunoresearch Laboratories, West Grove, PA) using the SNAP i.d. protein detection system (Millipore, Billerica, MA). The immunoreactive proteins were visualized with an ECL-plus kit (GE Healthcare Biosciences).

Duolink *in situ* PLA. Duolink *in situ* proximity ligation assay (PLA) reagents were obtained from OLINK Bioscience (Uppsala, Sweden). PC12 cells expressing GFP-JRAB/MICAL-L2 were fixed with 4% formaldehyde, permeabilized with 0.1% Triton X-100, and then blocked in 1× blocking stock (OLINK Bioscience). After incubation at room temperature with primary antibody for 1 h and secondary antibody conjugated with oligonucleotide for 2 h, assays were performed according to the manufacturer's instructions. The cells were observed with an Axiovert 200M imaging microscope (Carl Zeiss).

RESULTS

Effects of Rab13 mutants on neurite outgrowth in PC12 cells. Overexpression of Rab13 in PC12 cells has been shown to promote neurite outgrowth (4). Moreover, RNAi-based knockdown of Rab13 in PC12 cells resulted in marked reduction of neurite outgrowth in response to NGF treatment (4). To elucidate the mode of action of Rab13 during neurite outgrowth, we expressed a GFP-tagged constitutively active ("dominant active") Rab13 mutant (Rab13Q67L, Rab13DA), and a dominant negative Rab13 mutant (Rab13T22N, Rab13DN) in PC12 cells, and measured the longest neurite of each cell after staining with β-tubulin. In the absence of NGF, PC12 cells expressing GFP-Rab13DA displayed long neurites, whereas control cells expressing GFP showed few neurites (Fig. 1A). Remarkably, Rab13DA caused a considerable increase in the length of neurites (Fig. 1B). Expression of Rab13DN increased the number of cells showing a rounded morphology with few neurites, even in the presence of NGF, whereas the length of neurites was increased in control cells expressing GFP (Fig. 1C). The percentage of undifferentiated cells was increased in the GFP-Rab13DN-expressing cells (Fig. 1D). These results suggest that activation of Rab13 is correlated with neurite outgrowth in these cells.

Cooperation of Rab13 and JRAB/MICAL-L2 in neurite outgrowth. Previously, we identified JRAB/MICAL-L2 as a Rab13 effector protein and showed that Rab13 and JRAB/MICAL-L2 regulate epithelial plasticity through the transport of cell adhesion molecules (21, 24). We sought to examine whether the same system was involved in neurite outgrowth from PC12 cells. First, we produced a new anti-JRAB/MICAL-L2 antibody and evaluated it for investigation of JRAB/MICAL-L2 localization and expression in PC12 cells. To do this, we expressed Myc-tagged JRAB/MICAL-L2 in COS7 cells and confirmed that our new antibody specifically recognized the Myc-tagged JRAB/MICAL-L2 (Fig. 2Aa, left panel). Next, we examined whether the new antibody was suitable for immuno-

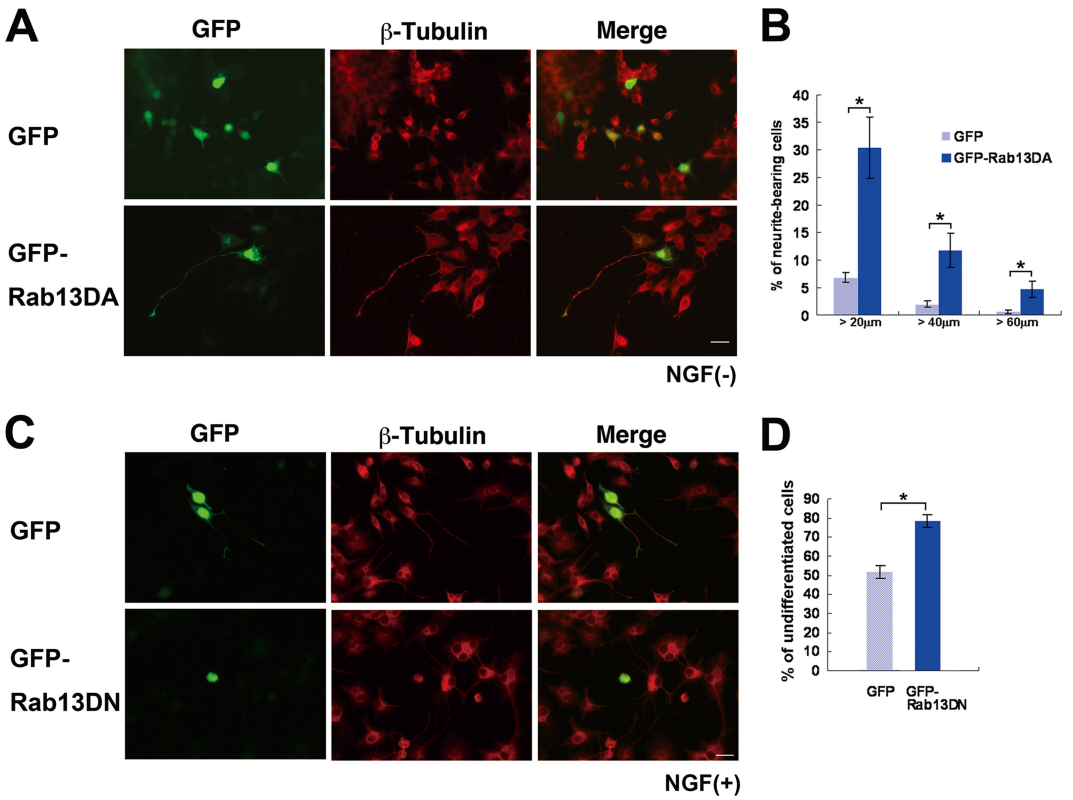

FIG. 1. The dominant active mutant of Rab13 induces neurite outgrowth in PC12 cells. (A) PC12 cells were transfected with an expression vector encoding GFP alone (GFP, upper panels) or GFP-tagged dominant active mutant of Rab13 (GFP-Rab13DA, lower panels). After 48 h, cells were fixed and immunostained with anti-β-tubulin antibody. Bar, 20 μm. (B) More than 100 transfected cells per experiment (random) were blindly selected, and the lengths of their neurites were measured by using ImageJ software (National Institutes of Health). The mean values (± the standard error) of the percentages of cells bearing neurites longer than 20, 40, or 60 μm from three independent experiments are shown. Statistical analyses were performed by analysis of variance (ANOVA) accompanied by a post-hoc Scheffe test. *, $P < 0.05$. (C) PC12 cells were transfected with an expression vector encoding GFP alone (GFP, upper panels) or GFP-tagged dominant negative mutant of Rab13 (GFP-Rab13DN, lower panels). Cells were visualized by immunostaining with an antibody against β-tubulin as described in panel A. Bar, 20 μm. (D) More than 100 transfected cells per experiment (random) were blindly selected, and the number of undifferentiated cells was determined. The histogram shows the percentage of undifferentiated cells in each group from three independent experiments. Statistical analyses were performed by using Student's *t* test. *, $P < 0.05$.

precipitation. The new antibody immunoprecipitated Myc-tagged JRAB/MICAL-L2 expressed in COS7 cells, but the control serum did not (Fig. 2Aa, right panel). We used this antibody to determine whether JRAB/MICAL-L2 is endogenously expressed in PC12 cells. Although endogenous JRAB/MICAL-L2 was not detected by immunoblotting of whole-cell lysates (data not shown), it was immunoprecipitated from PC12 cell lysates using our new antibody (Fig. 2Ab). We then used this antibody to characterize the localization of endogenous JRAB/MICAL-L2 in PC12 cells expressing GFP-Rab13DA. We found that JRAB/MICAL-L2 was concentrated in the perinuclear region and at the leading edge of extending neurites in PC12 cells expressing GFP-Rab13DA, whereas in the non-transfected cells it was localized to the perinuclear region only (Fig. 2B). We also confirmed that the staining for endogenous JRAB/MICAL-L2 was reduced by knockdown of JRAB/MICAL-L2 (Fig. 2F). Moreover, when PC12 cells were transfected with pEGFP vector containing wild-type Rab13 (Rab13WT), followed by treatment with NGF, we found that endogenous JRAB/MICAL-L2 was colocalized with GFP-Rab13WT in the perinuclear region and at the leading edge of NGF-induced neurites (Fig. 2C).

We next examined whether knockdown of JRAB/MICAL-L2 with RNA interference affected the neurite outgrowth of Rab13DA-expressed cells. We designed three siRNA oligomers targeting rat JRAB/MICAL-L2 (#1, #2, and #3). The siRNA oligomers were transfected into PC12 cells and 2 days after the transfection, mRNA expression was analyzed by real-time RT-PCR. siRNA #3 reduced the expression of JRAB/MICAL-L2 mRNA to ca. 10% of the levels seen in control siRNA-transfected cells. Next, to determine the effect of JRAB/MICAL-L2 knockdown on Rab13-mediated neurite outgrowth, we cotransfected siRNA #3 with pEGFP-Rab13DA into PC12 cells. We observed that JRAB/MICAL-L2 knockdown led to a reduction in the average neurite length in GFP-Rab13DA-positive, siRNA-transfected cells, compared to GFP-Rab13DA-positive, control siRNA-transfected cells (Fig. 2D). As to the effect of knockdown, there is a significant difference in the number of neurites longer than 20 or 40 μm between transfected and control cells (Fig. 2E). We also examined the

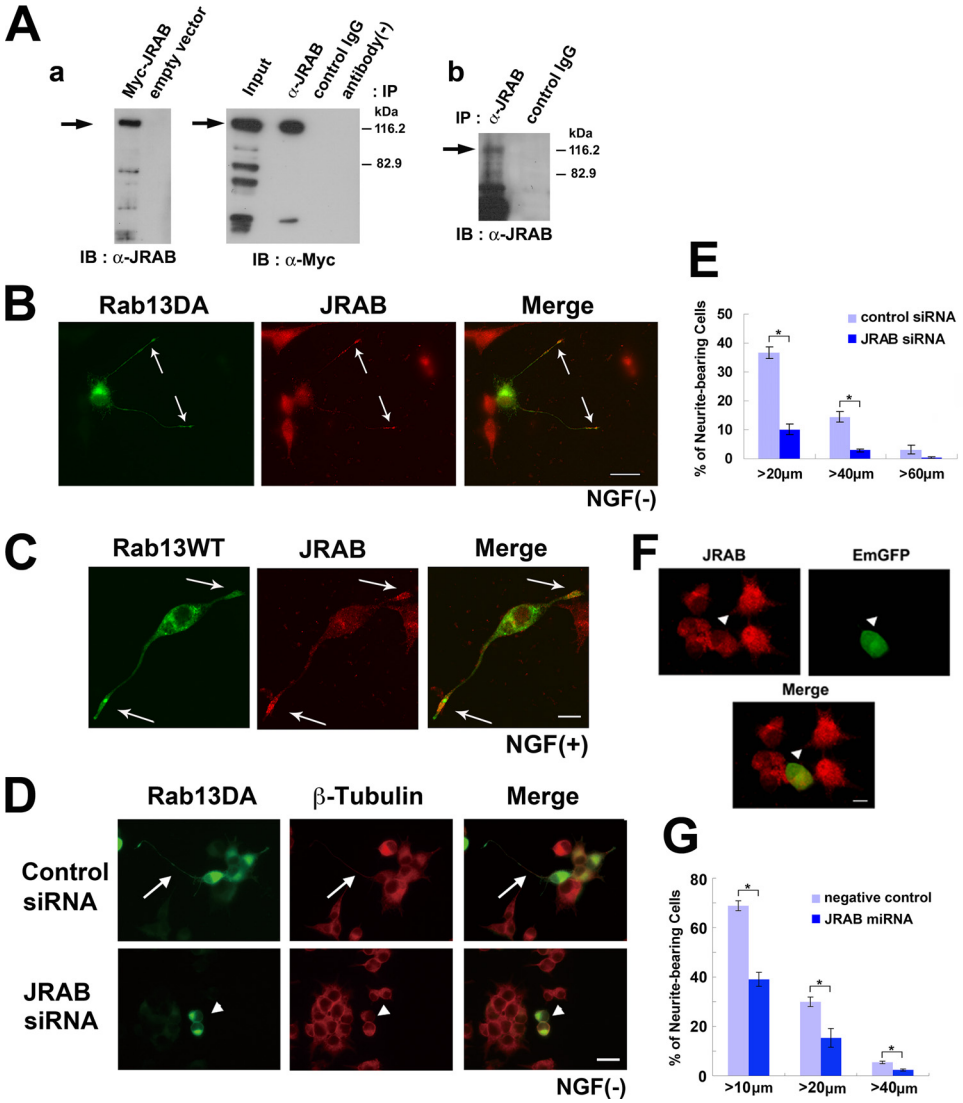

FIG. 2. JRAB/MICAL-L2 is required for Rab13-mediated neurite outgrowth in PC12 cells. (A) In subpanel a, left panel, COS7 cells were transfected with Myc-tagged JRAB/MICAL-L2 (lane 1) or empty vector (lane 2), lysed, and immunoblotted with an anti-JRAB/MICAL-L2 antibody. For the right panel, immunoprecipitation from the lysates of COS7 cells expressing Myc-tagged JRAB/MICAL-L2 (lane 1, input) was performed with an anti-JRAB/MICAL-L2 antibody (lane 2), control rabbit IgG (lane 3), or no antibody (lane 4). Immunoprecipitates were examined by immunoblotting with an anti-Myc antibody. In this blot, 5.5% of the total protein was loaded as an input. Subpanel b shows the expression of JRAB/MICAL-L2 in PC12 cells. Endogenous JRAB/MICAL-L2 was immunoprecipitated from PC12 cell lysates with an anti-JRAB/MICAL-L2 antibody (lane 1) but not with a control antibody (lane 2). An arrow indicates JRAB/MICAL-L2. (B) PC12 cells expressing GFP-Rab13DA were fixed, stained for JRAB/MICAL-L2 (red) with an anti-JRAB/MICAL-L2 antibody, and observed using fluorescence microscopy. GFP-Rab13DA and JRAB/MICAL-L2 were colocalized to the cell body and the tips of the neurites (arrows). Bar, 20 μm. (C) PC12 cells transfected with an expression vector encoding GFP-tagged wild-type Rab13 (GFP-Rab13WT) and treated with NGF were fixed and processed for immunostaining with an anti-JRAB/MICAL-L2 antibody (red). Endogenous JRAB/MICAL-L2 was mainly colocalized with GFP-Rab13WT in the perinuclear region and at the tips of the neurites (arrows). Bar, 10 μm. (D) PC12 cells were transfected with siRNA#3 or control siRNA combined with pEGFP-Rab13DA. siRNA#3 inhibited Rab13DA-mediated neurite outgrowth compared to control siRNA. Bar, 20 μm. (E) Quantification of neurite lengths in cells cotransfected with pEGFP-Rab13DA and siRNA#3 or control siRNA. Columns represent the percentage of cells bearing neurites longer than 20, 40, or 60 μm from three independent experiments ($n \geq 100$ per experiment). Statistical analyses were performed by ANOVA accompanied by a post-hoc Scheffe test. *, $P < 0.05$. (F) PC12 cells transfected with pcDNA6.2-GW/EmGFP-miR vector containing JRAB/MICAL-L2-directed miRNA insert, which was designed based on the target sequence of siRNA #3, were fixed and processed for immunostaining with an anti-JRAB/MICAL-L2 antibody (red). The staining of endogenous JRAB/MICAL-L2 was reduced in the transfected cells (arrowhead). Bar, 10 μm. (G) PC12 cells were transfected with pcDNA6.2-GW/EmGFP-miR-JRAB/MICAL-L2 #3 or pcDNA6.2-GW/EmGFP-miR-neg control plasmid, followed by treatment with NGF. The histogram shows the percentage of cells bearing neurites longer than 10, 20, or 40 μm from three independent experiments ($n \geq 100$ per experiment). Statistical analyses were performed by ANOVA accompanied by a post-hoc Scheffe test. *, $P < 0.05$.

effect of JRAB/MICAL-L2 knockdown on NGF-induced neurite outgrowth. PC12 cells were transfected with pcDNA6.2-GW/EmGFP-miR vector containing JRAB/MICAL-L2-directed miRNA insert, which was designed based on the target sequence of siRNA #3, followed by treatment with NGF. Knockdown of JRAB/MICAL-L2 was first confirmed by immunostaining analysis (Fig. 2F). The effect of JRAB/MICAL-L2 knockdown on neurite length could be clearly seen by compar-

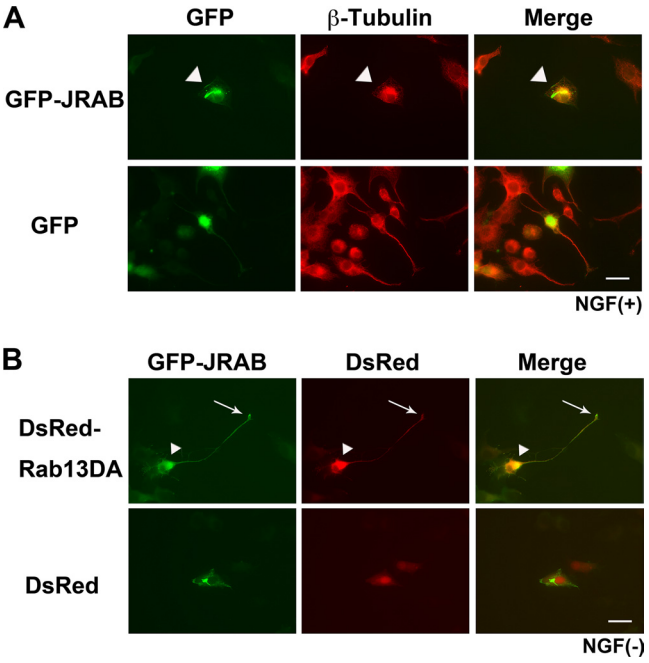

FIG. 3. Neurite outgrowth is inhibited by overexpressed JRAB/MICAL-L2 in PC12 cells. (A) PC12 cells transfected with pEGFP-JRAB/MICAL-L2 or pEGFP and treated with NGF were fixed and processed for immunostaining with an anti-β-tubulin antibody. GFP-JRAB/MICAL-L2 accumulated at the perinuclear region (arrowheads) and inhibited neurite outgrowth in all of the transfected cells (n = 266). Bar, 20 μm. (B) PC12 cells cotransfected with pEGFP-JRAB/MICAL-L2 and pDsRed-Rab13DA or pDsRed were fixed and processed for immunostaining with an anti-β-tubulin antibody. Cotransfection with pEGFP-JRAB/MICAL-L2 and pDsRed-Rab13DA led to neurite outgrowth (arrows) and disrupted the accumulation of GFP-JRAB/MICAL-L2 at the perinuclear region (n = 248). Bar, 20 μm.

ing the number of neurites longer than 10, 20, or 40 μm between JRAB/MICAL-L2-miRNA #3 and control-miRNA transfected cells (Fig. 2G). These results indicate that JRAB/MICAL-L2 is necessary for Rab13- and NGF-induced neurite outgrowth.

Exogenous expression of JRAB/MICAL-L2 inhibits neurite outgrowth. To further understand the function of JRAB/MICAL-L2 in neurite outgrowth, we expressed GFP-tagged JRAB/MICAL-L2 in PC12 cells and stained them with β-tubulin. Surprisingly, we often observed accumulation of GFP-JRAB/MICAL-L2 in the perinuclear region with no significant neurite outgrowth even in the presence of NGF (Fig. 3A). We then examined the effect of Rab13DA by transfecting pDsRed or pDsRed-Rab13DA together with pEGFP-JRAB/MICAL-L2 into PC12 cells. Fluorescence microscopic analyses demonstrated that overexpression of DsRed-Rab13DA rescued the GFP-JRAB/MICAL-L2-induced arrest of neurite formation, although that of DsRed alone did not (Fig. 3B). These results indicate that excess JRAB/MICAL-L2 has a specific inhibitory effect on neurite outgrowth, which is abolished by overexpression of Rab13DA.

The N-terminal region of JRAB/MICAL-L2 interacts with the C-terminal region. To explain the inhibitory effect of overexpressed JRAB/MICAL-L2 on neurite extension, we hypothesized that JRAB/MICAL-L2 is autoinhibited via an intramolecular interaction and that this interaction is overcome by binding of GTP-Rab13 to JRAB/MICAL-L2. To understand the relevance of this autoinhibition *in vitro*, we performed pulldown assays from COS7 cells expressing Myc-tagged JRAB-F (amino acids 1 to 1009), JRAB-N (amino acids 1 to 805) or JRAB-C (amino acids 806 to 1009) using recombinant GST-JRAB-C (Fig. 4Aa). These experiments revealed an interaction between GST-JRAB-C and Myc-JRAB-N, whereas no interactions were detectable between GST-JRAB-C and Myc-JRAB-F or between GST-JRAB-C and Myc-JRAB-C (Fig. 4Ab). These results suggest that the N-terminal region of JRAB/MICAL-L2 interacts intramolecularly with the C-terminal region.

The N-terminal CH and LIM domains contribute to interaction with the C-terminal region. The N-terminal region of JRAB/MICAL-L2 includes two domains, the calponin-homology (CH) domain (amino acids 3 to 102) and the LIM domain (amino acids 187 to 241) (21). To determine more specifically the site of interaction with JRAB-C, we prepared the following constructs (Fig. 4Ba): the CH domain alone (pCIneo-Myc JRAB-CH, amino acids 1 to 138), the LIM domain alone (pCIneo-Myc JRAB-LIM, amino acids 139 to 260), the CH domain and LIM domains together (pCIneo-Myc JRAB-CH+LIM, amino acids 1 to 260), and the MID domain (pCIneo-Myc JRAB-MID, amino acids 261 to 805). We measured the binding of the corresponding proteins to immobilized GST-JRAB-C in the pulldown assay. We found that Myc-tagged JRAB-CH+LIM bound very efficiently to GST-JRAB-C (Fig. 4Bb, left panel). Weak binding of Myc-JRAB-LIM to GST-JRAB-C was also observed. However, no interactions between GST-JRAB-C and Myc-JRAB-CH or Myc-JRAB-MID were detectable (Fig. 4Bb, left panel). In control experiments, none of the constructs bound to GST alone (Fig. 4Bb, right panel). These results demonstrate that the CH+LIM domain (and particularly the LIM domain) may be the minimal domain responsible for the intramolecular interaction of the N- and C-terminal regions of JRAB/MICAL-L2.

The C-terminal region lacking the coiled-coil (CC) domain interacts with Rab13. Previously, we showed that GTP-Rab13 interacts with the C-terminal region of JRAB/MICAL-L2 (amino acids 806 to 1009) (21, 24). We next sought to examine whether this interaction competes with the intramolecular interaction within JRAB/MICAL-L2. COS7 cells were transfected with expression vectors for Myc-tagged JRAB-CH+LIM or GFP-tagged Rab13DA. Lysates were subjected to the same pulldown assay as before using GST-JRAB-C and other truncation mutants. These mutants were designed to contain or exclude the CC domain of the C-terminal region of JRAB/MICAL-L2 (JRAB-CC, amino acids 806 to 912, and JRAB-CT, amino acids 913 to 1009, respectively; see Fig. 4Ca). The results of the pulldown assay revealed that the CC domain is the site of JRAB-CH+LIM binding, whereas the CT domain participates in the Rab13DA interaction (Fig. 4Cb), indicating that the GTP-Rab13- and JRAB-CH+LIM-interacting domains are separable.

Intramolecular interaction of JRAB/MICAL-L2 in PC12 cells. Finally, we analyzed the intramolecular interaction of JRAB/MICAL-L2 in PC12 cells using Duolink *in situ* PLA. This assay system consists of a pair of oligonucleotide-labeled secondary antibodies (PLA probes). A signal is generated only

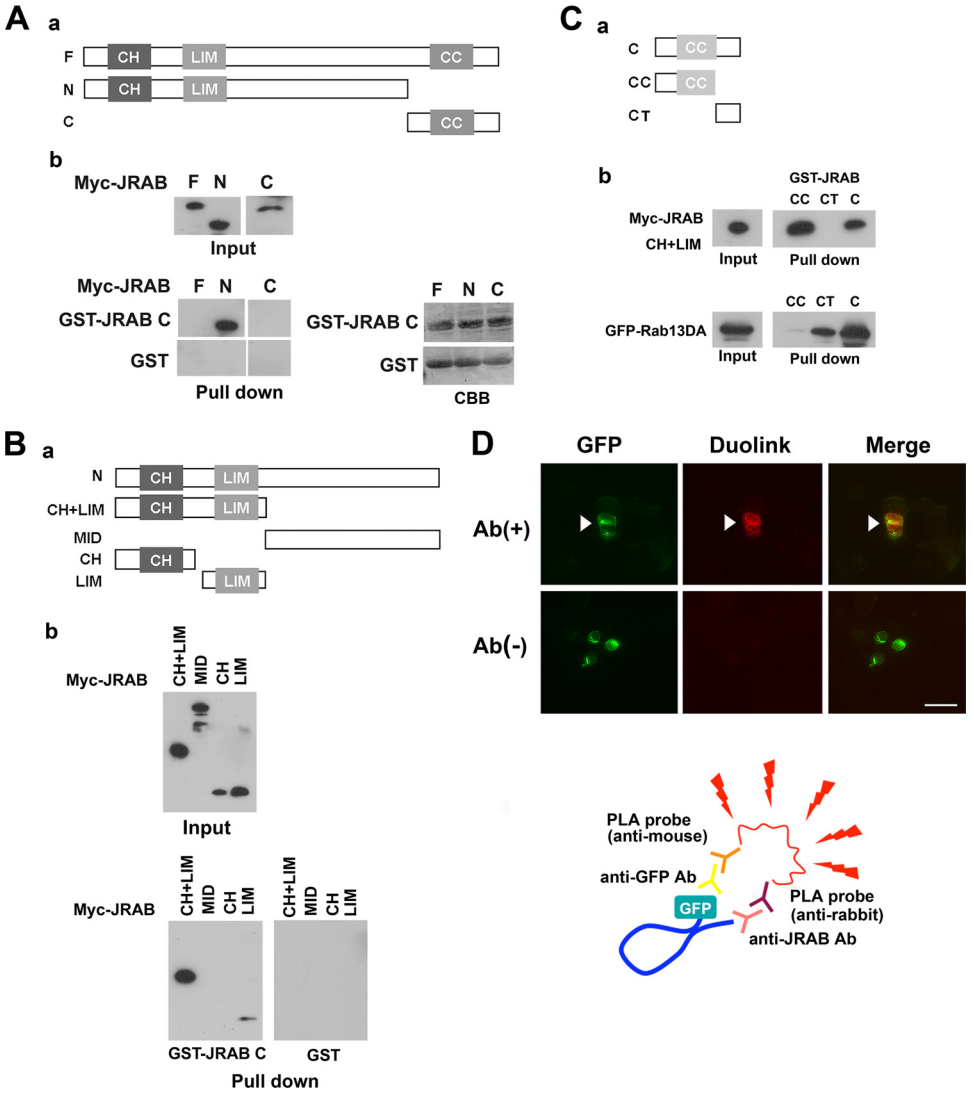

FIG. 4. Intramolecular interaction between the N-terminal and C-terminal regions of JRAB/MICAL-L2. (A) The N-terminal region of JRAB/MICAL-L2 interacts with its C-terminal region. (a) Structures of the full-length JRAB/MICAL-L2 (row F) and JRAB/MICAL-L2 mutants: JRAB-N (row N) and JRAB-C (row C). JRAB/MICAL-L2 is composed of the CH domain (CH, amino acids 3 to 102), the LIM domain (LIM, amino acids 131 to 260), and the CC domain (CC, amino acids 806 to 912). (b) Pulldown assay. COS7 cells expressing Myc-tagged JRAB/MICAL-L2 constructs (F, N, and C) were lysed and subjected to pulldown assay with GST-JRAB-C. Bound proteins were detected by immunoblotting with an anti-Myc antibody. CBB indicates the Coomassie brilliant blue staining of GST-JRAB-C and GST used for the assays. Myc-JRAB-N bound to GST-JRAB-C, but Myc-JRAB-F and -JRAB-C did not. (B) The CH+LIM domain of JRAB/MICAL-L2 interacts with its C-terminal region. (a) Structures of various fragments of JRAB-N. (b) COS7 cells expressing the indicated truncated mutants (CH+LIM, MID, CH, and LIM) were lysed and subjected to the pulldown assay using GST-JRAB-C. Bound proteins were detected by immunoblotting with an anti-Myc antibody. Myc-JRAB-CH+LIM and -LIM bound to GST-JRAB-C, but Myc-JRAB-CH and -MID did not. (C) The Rab13- and JRAB-CH+LIM-interacting domains were separable. (a) Structures of various fragments of JRAB-C. (b) COS7 cells expressing Myc-JRAB-CH+LIM or GFP-Rab13DA were lysed and subjected to the pulldown assay using GST-JRAB-C, -CC, or -CT. The bound proteins were detected by immunoblotting with anti-Myc and anti-GFP antibodies. Myc-JRAB-CH+LIM bound to GST-JRAB-C and -CC, whereas GFP-Rab13DA bound to GST-JRAB-C and -CT. (D) Intramolecular interaction of JRAB/MICAL-L2 was observed by Duolink assay in PC12 cells. PC12 cells transfected with GFP-JRAB/MICAL-L2 were fixed and subjected to Duolink *in situ* PLA. The assays were performed with an anti-GFP antibody in the presence [Ab(+)] or absence [Ab(−)] of an anti-JRAB/MICAL-L2 antibody. An arrowhead in the upper panel indicates a positive signal. Bar, 20 μm. The schematic illustrates the principle of the Duolink *in situ* PLA; the anti-GFP and anti-JRAB/MICAL-L2 antibodies bound to GFP-JRAB/MICAL-L2 expressed in PC12 cells in close proximity, producing the positive signal.

when the two PLA probes bind to two primary antibodies that have bound to the sample in close proximity. For this assay, we expressed GFP-JRAB/MICAL-L2 in PC12 cells and used rabbit anti-JRAB/MICAL-L2 and mouse anti-GFP antibodies. The anti-JRAB/MICAL-L2 antibody was generated by GST-JRAB-C. Therefore, if the N-terminal and C-terminal regions of JRAB/MICAL-L2 interacted in PC12 cells as observed in the pulldown assay, the anti-GFP and anti-JRAB/MICAL-L2 antibodies would bind to JRAB/MICAL-L2 in close proximity (see schematic in Fig. 4D). We observed a signal when GFP-

JRAB/MICAL-L2 was expressed in PC12 cells (Fig. 4D, upper panels). In contrast, we observed no signal in the absence of anti-JRAB/MICAL-L2 antibody (Fig. 4D, lower panels). These results also support a model in which JRAB/MICAL-L2 interacts with itself intramolecularly in PC12 cells.

JRAB/MICAL-L2ΔCT mutant inhibits neurite outgrowth. Next, to examine whether the binding of GTP-Rab13 to JRAB/MICAL-L2 is associated with release from the intramolecular interaction, we constructed a GFP-tagged JRAB/MICAL-L2 which lacked the Rab13-binding CT domain (GFP-JRAB/MICAL-L2ΔCT) and examined its effect on neurite outgrowth. When GFP-JRAB/MICAL-L2ΔCT was expressed in PC12 cells, accumulation of JRAB/MICAL-L2ΔCT was observed in the perinuclear region and no significant induction of neurite outgrowth was observed in the presence of NGF (Fig. 5A). We then examined the effect of Rab13DA on this process. In contrast to GFP-JRAB/MICAL-L2 (Fig. 3B), Rab13DA did not rescue the inhibitory effect of JRAB/MICAL-L2ΔCT on neurite outgrowth (Fig. 5B). These immunocytochemical data suggest that JRAB/MICAL-L2ΔCT still interacts with itself intramolecularly and that GTP-Rab13 could not release this interaction. Actually, when Myc-JRAB/MICAL-L2ΔCT was expressed in COS7 cells and subjected to the pulldown assay using GST-JRAB-C, it was not pulled down (Fig. 5C). These results suggest that the binding of GTP-Rab13 to JRAB/MICAL-L2 may be important for neurite outgrowth through the release of JRAB/MICAL-L2 from intramolecular interaction. We further confirmed this model by use of Duolink *in situ* PLA. GFP-Rab13DA was expressed in PC12 cells and the Duolink assay was performed with anti-GFP and anti-JRAB/MICAL-L2 antibodies. Signals were detected at both the perinuclear region and the neurites (Fig. 5D), indicating that GFP-Rab13DA interacts with endogenous JRAB/MICAL-L2 in the perinuclear region and along the Rab13-mediated neurite extensions.

JRAB/MICAL-L2ΔCC mutant does not inhibit neurite outgrowth. We next examined whether the release from the intramolecular interaction is determinant for the function of JRAB/MICAL-L2. For this purpose, we constructed JRAB/MICAL-L2ΔCC lacking the CC domain and examined the intramolecular interaction and its effect on neurite outgrowth. When Myc-tagged JRAB/MICAL-L2ΔCC was expressed in COS7 cells and subjected to the pulldown assay using GST-JRAB-C, it was pulled down as well as Myc-tagged JRAB-N (Fig. 6A). Moreover, when GFP-JRAB/MICAL-L2ΔCC was expressed in PC12 cells, accumulation of GFP-JRAB/MICAL-L2ΔCC did not occur at all, in contrast to GFP-JRAB/MICAL-L2 (Fig. 3B) and small neurites were observed (Fig. 6B). We then examined the effect of Rab13DA on this process. Coexpression of Rab13DA with GFP-JRAB/MICAL-L2ΔCC resulted in more robust stimulation of the neurite outgrowth (Fig. 6C). These results suggest that the release of intramolecular interaction is essential but not sufficient for neurite outgrowth.

Effect of JRAB/MICAL-L2 and JRAB/MICAL-L2ΔCT on reorganization of the actin cytoskeleton. It has been well established that reorganization of the cytoskeleton, including microtubules and F-actin, plays a crucial role in neurite outgrowth and the navigation of growth cones (2, 12). Therefore, it seemed likely that the inhibitory effect of GFP-JRAB/MICAL-L2 on neurite outgrowth was associated with cytoskeletal disorganization. As shown in Fig. 3A, the microtubule architecture was not drastically changed in the cell body, although the neurites were not extended. We previously showed that JRAB/MICAL-L2 was colocalized with F-actin in NIH

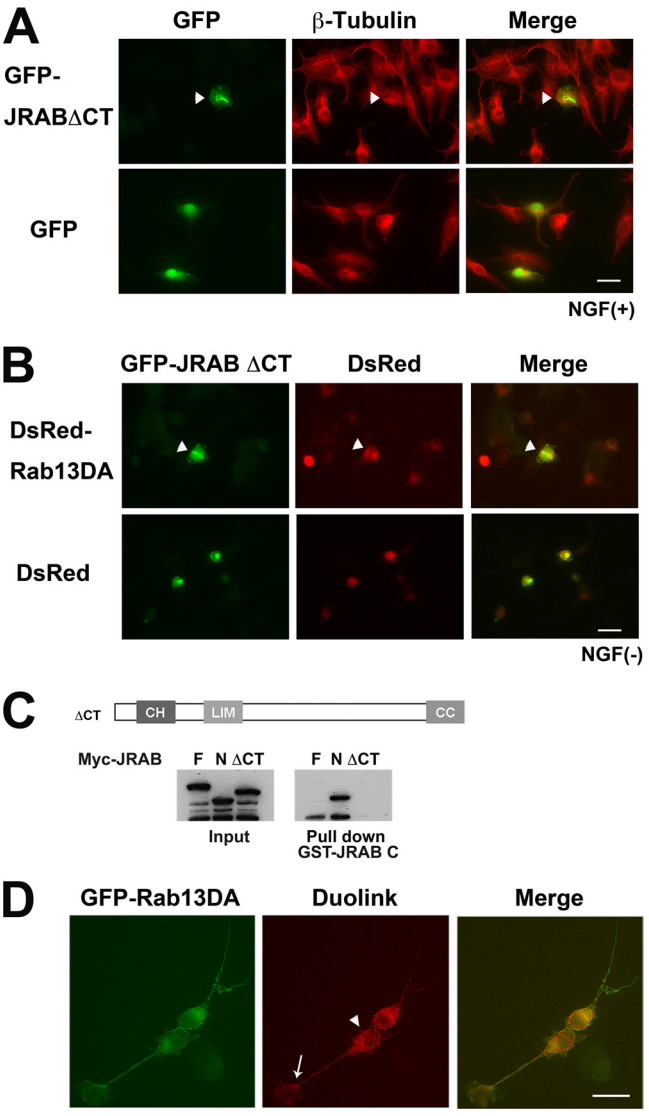

FIG. 5. The JRABΔCT mutant inhibits Rab13-mediated neurite outgrowth in PC12 cells. (A) PC12 cells were transfected with either pEGFP-JRABΔCT or pEGFP and stimulated with NGF for 2 days, followed by immunostaining for β-tubulin. Accumulation of GFP-JRABΔCT (arrowheads) was observed in all of the transfected cells (n = 279). Bar, 20 μm. (B) PC12 cells cotransfected with pEGFP-JRABΔCT and pDsRed-Rab13DA or pDsRed were observed by direct GFP or DsRed fluorescence ($n \geq 100$ per experiment). Bar, 20 μm. (C) Schematic of the structure of JRABΔCT, lacking the CT domain (amino acids 913 to 1009). COS7 cells expressing Myc-JRAB-F, -N, or -ΔCT were lysed and subjected to the pulldown assay using GST-JRAB-C. Neither Myc-JRABΔCT nor Myc-JRAB-F bound to GST-JRAB-C, whereas Myc-JRAB-N did. (D) PC12 cells transfected with GFP-Rab13DA were fixed and subjected to the Duolink *in situ* PLA. The assay was performed with anti-GFP and anti-JRAB/MICAL-L2 antibodies. A positive signal was observed in both the cell body (arrowhead) and neurites (arrow). Bar, 20 μm.

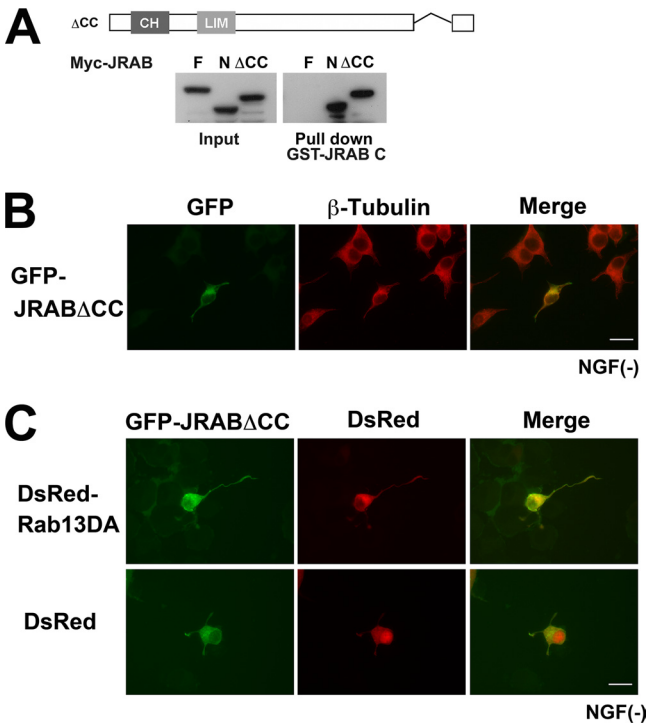

FIG. 6. Effect of JRABΔCC mutant on neurite outgrowth in PC12 cells. (A) Schematic of the structure of JRABΔCC, lacking the CC domain (amino acids 806 to 912). COS7 cells expressing Myc-JRAB-F, -N, or -ΔCC were lysed and subjected to the pulldown assay using GST-JRAB-C. Either Myc-JRABΔCC or Myc-JRAB-N bound to GST-JRAB-C, whereas Myc-JRAB-F did not. (B) PC12 cells were transfected with pEGFP-JRABΔCC and immunostained with anti-β-tubulin antibody. Accumulation of GFP-JRABΔCC was not observed in all of the transfected cells (n = 198). Bar, 20 μm. (C) PC12 cells cotransfected with pEGFP-JRABΔCC and pDsRed-Rab13DA or pDsRed were observed by direct GFP or DsRed fluorescence ($n \geq 100$ per experiment). Bar, 20 μm.

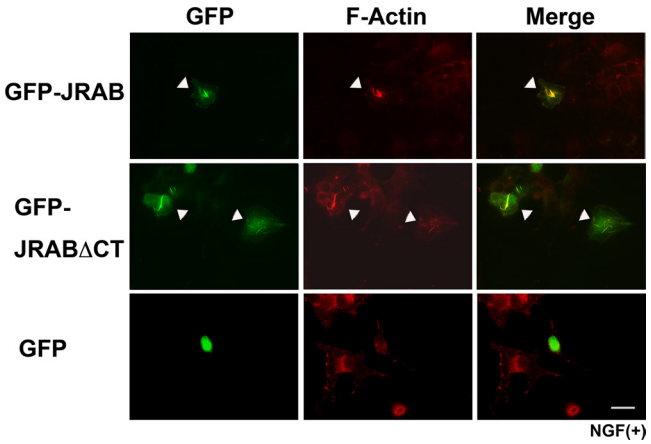

FIG. 7. Effect of JRAB/MICAL-L2 on actin cytoskeletal rearrangement during neurite outgrowth in PC12 cells. PC12 cells transfected with pEGFP-JRAB/MICAL-L2, pEGFP-JRABΔCT, or pEGFP were fixed and processed for double fluorescence to visualize the actin filaments by direct GFP fluorescence detection and indirect immunofluorescence detection using rhodamine-phalloidin. GFP-JRAB/MICAL-L2 and GFP-JRABΔCT (arrows) were accumulated in the perinuclear region and costained with phalloidin in all of the transfected cells ($n \geq 100$ per experiment). Bar, 20 μm.

3T3 cells (21). We sought to examine the effect of JRAB/MICAL-L2 expression on the reorganization of the actin cytoskeleton in PC12 cells. In differentiated PC12 cells, the tips of the neurites and the small spikes were stained with rhodamine phalloidin, and faint staining was also observed throughout the cell body (Fig. 7, lower panels). When PC12 cells expressing GFP-JRAB/MICAL-L2 were stained with rhodamine phalloidin, the GFP-JRAB/MICAL-L2-positive compartments in the perinuclear region were strongly costained with phalloidin (Fig. 7, upper panels). Similarly, when GFP-JRAB/MICAL-L2ΔCT was expressed in PC12 cells, GFP-JRAB/MICAL-L2ΔCT was found accumulated in the perinuclear region as described above and was costained with phalloidin (Fig. 7, middle panels). These results indicate that expression of JRAB/MICAL-L2 or JRAB/MICAL-L2ΔCT induced the accumulation of F-actin and that both proteins colocalized with this accumulated F-actin, suggesting that this actin cytoskeletal change might cause the inhibitory effect on neurite outgrowth.

Involvement of Rab13-JRAB/MICAL-L2-actinin-4 in neurite outgrowth. Previously, we showed that actinin-4, an actin-binding protein, binds to JRAB/MICAL-L2, and that this interaction is enhanced by Rab13 activation (15). We sought to determine whether actinin-4 is involved in Rab13-induced neurite outgrowth. We first confirmed the expression of actinin-4 in PC12 cells by immunoblotting (data not shown). We observed that actinin-4 was intracellularly localized throughout the cytoplasm of the soma, and especially to the short spikelike structures protruding from the somata (Fig. 8A, lower panels). When GFP-Rab13DA was expressed in PC12 cells, actinin-4 was concentrated at the tip of the Rab13DA-induced neurites as well as in the cytoplasm of the soma (Fig. 8A, upper panels). These observations were confirmed by transfection of pEGFP-actinin-4 and pDsRed-Rab13DA (data not shown). Next, we examined whether actinin-4 was colocalized with Rab13 and JRAB/MICAL-L2. When GFP-Rab13DA and Myc-actinin-4 were expressed in PC12 cells, endogenous JRAB/MICAL-L2 was colocalized with GFP-Rab13DA in the perinuclear region and along the neurites, where the most prominent staining was observed at the tip (Fig. 8B). Similarly, Myc-actinin-4 was also colocalized with these proteins at both sites. Because these observations were not sufficient to determine whether JRAB/MICAL-L2 interacted with actinin-4 at these sites, we performed further assays using Duolink *in situ* PLA. GFP-Rab13DA and Myc-actinin-4 were expressed in PC12 cells, and the Duolink assay was performed with anti-JRAB/MICAL-L2 and anti-Myc antibodies. Signals were detected at both the perinuclear region and the neurites (Fig. 8C), indicating that endogenous JRAB/MICAL-L2 interacted with actinin-4 at both sites. To confirm the finding of interaction, GFP-JRAB/MICAL-L2 was then coexpressed with HA-Rab13DA and Myc-actinin-4, and the Duolink assay was performed with anti-GFP and anti-Myc antibodies. The cells expressing the three proteins showed clear signals in the cell body and the tips of the neurites (Fig. 8D). These results suggest a role in neurite outgrowth for the Rab13-induced interaction of JRAB/MICAL-L2 with actinin-4.

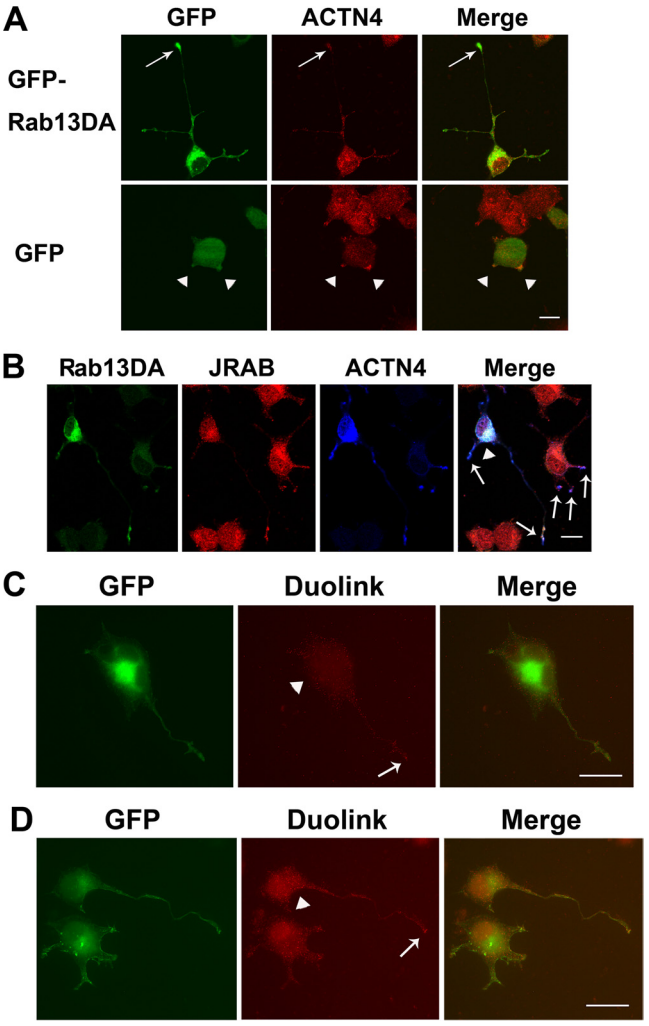

FIG. 8. Rab13-JRAB/MICAL-L2-actinin-4 is involved in neurite outgrowth in PC12 cells. (A) PC12 cells transfected with pEGFP-Rab13DA or pEGFP were fixed and stained with an anti-actinin-4 antibody. Actinin-4 was colocalized with GFP-Rab13DA in both the cell body and the tips of the Rab13-induced neurites (arrows). Bar, 20 μm. (B) PC12 cells cotransfected with pEGFP-Rab13DA and pCIneo-Myc-actinin-4 were fixed and stained with anti-JRAB/MICAL-L2 and anti-Myc antibodies. Actinin-4 was colocalized with GFP-Rab13DA and JRAB/MICAL-L2 in both the cell body (arrowhead) and the tips of the Rab13-induced neurites (arrows). Bar, 20 μm. (C) PC12 cells cotransfected with pEGFP-Rab13DA and pCIneo-Myc-actinin-4 were fixed and subjected to the Duolink assay. The assay was performed with anti-Myc and anti-JRAB/MICAL-L2 antibodies. A positive signal was observed in both the cell body (arrowhead) and neurites (arrow). Bar, 20 μm. (D) PC12 cells cotransfected with pCIneo-HA-Rab13DA, pEGFP-JRAB/MICAL-L2 and pCIneo-Myc-actinin-4 were fixed and subjected to the Duolink assay. The assay was performed with anti-Myc and anti-GFP antibodies. The signal was stronger than that observed in panel C. Bar, 20 μm.

DISCUSSION

In our previous studies, we proposed a role for Rab13-JRAB/MICAL-L2 in the establishing of cell-cell adhesion and cell polarization in epithelial cells, via the transport of adhesion molecules, claudins and occludin (14, 16, 21, 24). In addition, Di Giovanni et al. reported that Rab13 mRNA expression is increased after spinal cord injury, suggesting that it is involved in nerve regeneration (4). Therefore, we suggest that Rab13-JRAB/MICAL-L2 might function as a key regulator of a general mechanism for cell polarization not only in epithelial cells but also in neuronal cells. In epithelial cells, claudins and occludin were identified as components of tight junction strands; they contribute to cell-cell adhesion. However, neuronal cells do not have tight junctions at the cell-cell adhesion sites and have an intrinsic deficiency in both claudins and occludin. Thus, it may be speculated that Rab13-JRAB/MICAL-L2 is involved in the transport of other neuronal cell adhesion molecules or receptors to the synapses for synaptic formation and/or to the tip of developing neurites for neuritogenesis.

In the present study, we first showed that the expression of a constitutively active Rab13 mutant promoted neurite outgrowth from PC12 cells without NGF stimulation, whereas a dominant negative Rab13 mutant inhibits it even in the presence of NGF. These results suggest that activation of Rab13 is necessary for NGF-induced neurite outgrowth from PC12 cells. In addition, we speculate that Rab13 may be activated by NGF signaling. We previously showed by pulldown assay using GST-tagged Rab13-binding C-terminal domain of JRAB/MICAL-L2 that Rab13 is transiently activated in MDCK cells during phorbol ester-induced cell scattering (9). Using this method, we tried to show the activation of Rab13 induced by NGF in PC12 cells, but we could not prove this point because of the inability of our antibody to detect rat Rab13. We moreover found that knockdown of JRAB/MICAL-L2 expression inhibits Rab13- and NGF-mediated neurite elongation. These observations suggest that the Rab13-JRAB/MICAL-L2 pathway is involved in NGF-mediated neurite outgrowth. However, overexpression of JRAB/MICAL-L2 alone results in accumulation at the perinuclear region and round cell morphology, whereas coexpression of a constitutively active mutant of Rab13 rescues this effect. Hence, our findings support an attractive hypothesis: that Rab13-JRAB/MICAL-L2 regulates neurite outgrowth by maintaining a fine balance. We suggest as a possible molecular mechanism that JRAB/MICAL-L2 might have "open" and "closed" conformations. In this case, a conformational change could be induced by an interaction with GTP-Rab13, which might be similar to that described for the Rho family of small G proteins and their effector proteins (1, 10, 11, 19). For example, N-WASP, which is implicated in filopodia formation downstream of Cdc42, shows intramolecular interaction between the N-terminal domain and the C-terminal effector domain. This interaction inhibits the activity of the effector domain, which regulates actin nucleation. Binding of Cdc42 to N-WASP reduces the affinity of the N-WASP intramolecular interaction and changes its conformation from "closed" to "open," leading to release from the inhibitory effect.

Interestingly, the pulldown assay using the GST-tagged C-terminal domain of JRAB/MICAL-L2, containing the CC and CT domain, revealed that the JRAB/MICAL-L2 N-terminal mutant lacking the C-terminal domain can bind to the fusion protein, but the full-length protein cannot. The JRAB/MICAL-L2 N-terminal region contains the CH domain and LIM domain (21, 22). In addition, we determined that the LIM domain is mainly responsible for binding to the C-terminal region. Moreover, two different parts of the JRAB/MICAL-L2

C-terminal region, CC and CT, bind to the JRAB/MICAL-L2 N-terminal region containing the CH+LIM domain and GTP-Rab13, respectively, indicating that the binding sites of Rab13 and the JRAB/MICAL-L2 N-terminal region to JRAB/MICAL-L2 C-terminal region are separable. These observations raise the possibility that the functional activity of JRAB/MICAL-L2 is autoinhibited by an intramolecular interaction between the CH+LIM and CC domains and that the binding of GTP-Rab13 to the CT domain leads to a conformational change of JRAB/MICAL-L2 that removes this inhibition. Further support for this notion comes from the observation that the JRAB/MICAL-L2ΔCT mutant lacking the Rab13 binding domain, which might be stable in the "closed" conformation, was not able to interact with the JRAB/MICAL-L2 C-terminal domain, and inhibited the induction of neurite elongation as well as the full-length protein, but with no recovery after expression of the dominant active form of Rab13. In contrast, the JRAB/MICAL-L2ΔCC mutant lacking CC domain, which might be stable in the "open" conformation, stimulated neurite outgrowth in the absence of NGF, but its effect was smaller than that of Rab13DA. These results suggest that Rab13DA not only induces conformational change of JRAB/MICAL-L2 to make "open" form but also transports it to the functional sites, especially the tip of the neurites and that both actions of Rab13 are necessary for the function of JRAB/MICAL-L2. Further study including the crystal structural analysis will be necessary for elucidating the precise mode of action of Rab13-JRAB/MICAL-L2 in neurite outgrowth.

The mechanisms regulating actin cytoskeletal rearrangement during neurite outgrowth have been well characterized (2, 12, 17). In contrast, the molecular cascade leading to the accumulation of the many molecules involved in actin dynamics at the tips of neurites is largely uncharacterized. In this light, our observation that overexpression of JRAB/MICAL-L2 induces accumulation of F-actin and JRAB/MICAL-L2 itself at the perinuclear region and inhibits neurite elongation is particularly intriguing. Of great interest would be the link between JRAB/MICAL-L2 and the actin cytoskeletal rearrangement, which results in the formation of neurites. We have recently shown that actinin-4, an actin-binding protein, binds to JRAB/MICAL-L2 and that the interaction is enhanced by Rab13 activation (15). Actinin-4 could play a role in Rab13-JRAB/MICAL-L2-mediated neurite outgrowth, in light of the results reported here, that actinin-4 is associated with the dominant active form of Rab13 and JRAB/MICAL-L2 at the tip of the growing neurites in addition to the perinuclear region. The tips of the neurites consist of dynamic finger-like filopodia that "explore the road ahead" (12). These structures are formed by F-actin bundles, which may be constructed by actinin-4. A likely explanation of our findings would be that Rab13 induces the interaction of JRAB/MICAL-L2 with actinin-4 and that their complex is transported to the leading edge by Rab13, resulting in the formation of the fingerlike filopodia that are important for neurite outgrowth. However, unidentified JRAB/MICAL-L2-interacting protein(s) should not be ruled out as possible mechanisms of this action.

In any case, the Rab13-JRAB/MICAL-L2-dependent actin cytoskeletal rearrangement described here could also be coordinated by signaling from molecule(s) transferred by Rab13-mediated vesicle transport. However, the candidate molecules on Rab13-containing vesicles remain unknown. Therefore, it is critically important to identify the cargo proteins of Rab13-JRAB/MICAL-L2-mediated transport in neurons. Future investigations should aim to elucidate the details of the molecular mechanism linking the actin cytoskeletal rearrangement to this complex molecular network.

ACKNOWLEDGMENTS

We thank Takashi Matozaki and Hiroshi Ohnishi (Gunma University, Gunma, Japan) for their advice and suggestions. We also thank Hiroyoshi Sei (University of Tokushima) for helping with the statistical analyses.

This study was supported by Grants-in-Aid for Scientific Research (T.S., 2009), for Scientific Research on Innovative Areas (T.S., 2008 and 2009), and for Young Scientists (A.S., 2008 and 2009) from the Ministry of Education, Culture, Sports, Science, and Technology of Japan; the Naito Foundation (T.S., 2009); and Inoue Research Aid for Young Scientists (A.S., 2007).

REFERENCES

1. **Buck, M., W. Xu, and M. K. Rosen.** 2004. A two-state allosteric model for autoinhibition rationalizes WASP signal integration and targeting. J. Mol. Biol. **338:**271–285.
2. **Dent, E. W., and F. B. Gertler.** 2003. Cytoskeletal dynamics and transport in growth cone motility and axon guidance. Neuron **40:**209–227.
3. **Dickson, B. J.** 2001. Rho GTPases in growth cone guidance. Curr. Opin. Neurobiol. **11:**103–110.
4. **Di Giovanni, S., A. De Biase, A. Yakovlev, T. Finn, J. Beers, E. P. Hoffman, and A. I. Faden.** 2005. In vivo and in vitro characterization of novel neuronal plasticity factors identified following spinal cord injury. J. Biol. Chem. **280:** 2084–2091.
5. **Etienne-Manneville, S., and A. Hall.** 2002. Rho GTPases in cell biology. Nature **420:**629–635.
6. **Hall, A.** 1998. Rho GTPases and the actin cytoskeleton. Science **279:**509–514.
7. **Honda, K., T. Yamada, Y. Hayashida, M. Idogawa, S. Sato, F. Hasegawa, Y. Ino, M. Ono, and S. Hirohashi.** 2005. Actinin-4 increases cell motility and promotes lymph node metastasis of colorectal cancer. Gastroenterology **128:**51–62.
8. **Jaffe, A. B., and A. Hall.** 2005. Rho GTPases: biochemistry and biology. Annu. Rev. Cell Dev. Biol. **21:**247–269.
9. **Kanda, I., N. Nishimura, H. Nakatsuji, R. Yamamura, H. Nakanishi, and T. Sasaki.** 2008. Involvement of Rab13 and JRAB/MICAL-L2 in epithelial cell scattering. Oncogene **27:**1687–1695.
10. **Lammers, M., R. Rose, A. Scrima, and A. Wittinghofer.** 2005. The regulation of mDia1 by autoinhibition and its release by Rho*GTP. EMBO J. **24:**4176–4187.
11. **Li, F., and H. N. Higgs.** 2003. The mouse Formin mDia1 is a potent actin nucleation factor regulated by autoinhibition. Curr. Biol. **13:**1335–1340.
12. **Lowery, L. A., and D. Van Vactor.** 2009. The trip of the tip: understanding the growth cone machinery. Nat. Rev. Mol. Cell. Biol. **10:**332–343.
13. **Luo, L.** 2000. Rho GTPases in neuronal morphogenesis. Nat. Rev. Neurosci. **1:**173–180.
14. **Morimoto, S., N. Nishimura, T. Terai, S. Manabe, Y. Yamamoto, W. Shinahara, H. Miyake, S. Tashiro, M. Shimada, and T. Sasaki.** 2005. Rab13 mediates the continuous endocytic recycling of occludin to the cell surface. J. Biol. Chem. **280:**2220–2228.
15. **Nakatsuji, H., N. Nishimura, R. Yamamura, H. O. Kanayama, and T. Sasaki.** 2008. Involvement of actinin-4 in the recruitment of JRAB/MICAL-L2 to cell-cell junctions and the formation of functional tight junctions. Mol. Cell. Biol. **28:**3324–3335.
16. **Nishimura, N., and T. Sasaki.** 2009. Rab family small G proteins in regulation of epithelial apical junctions. Front. Biosci. **14:**2115–2129.
17. **Pak, C. W., K. C. Flynn, and J. R. Bamburg.** 2008. Actin-binding proteins take the reins in growth cones. Nat. Rev. Neurosci. **9:**136–147.
18. **Prochiantz, A.** 1995. Neuronal polarity: giving neurons heads and tails. Neuron **15:**743–746.
19. **Suetsugu, S., H. Miki, and T. Takenawa.** 2001. Identification of another actin-related protein (Arp) 2/3 complex binding site in neural Wiskott-Aldrich syndrome protein (N-WASP) that complements actin polymerization induced by the Arp2/3 complex activating (VCA) domain of N-WASP. J. Biol. Chem. **276:**33175–33180.

20. **Takai, Y., T. Sasaki, and T. Matozaki.** 2001. Small GTP-binding proteins. Physiol. Rev. **81:**153–208.
21. **Terai, T., N. Nishimura, I. Kanda, N. Yasui, and T. Sasaki.** 2006. JRAB/MICAL-L2 is a junctional Rab13-binding protein mediating the endocytic recycling of occludin. Mol. Biol. Cell **17:**2465–2475.
22. **Terman, J. R., T. Mao, R. J. Pasterkamp, H. H. Yu, and A. L. Kolodkin.** 2002. MICALs, a family of conserved flavoprotein oxidoreductases, function in plexin-mediated axonal repulsion. Cell **109:**887–900.
23. **Wiggin, G. R., J. P. Fawcett, and T. Pawson.** 2005. Polarity proteins in axon specification and synaptogenesis. Dev. Cell **8:**803–816.
24. **Yamamura, R., N. Nishimura, H. Nakatsuji, S. Arase, and T. Sasaki.** 2008. The interaction of JRAB/MICAL-L2 with Rab8 and Rab13 coordinates the assembly of tight junctions and adherens junctions. Mol. Biol. Cell **19:**971–983.
25. **Zerial, M., and H. McBride.** 2001. Rab proteins as membrane organizers. Nat. Rev. Mol. Cell. Biol. **2:**107–117.